

Article

HDL quality features revealed by proteome–lipidome connectivity are associated with atherosclerotic disease

Dandan Wang^{1,†}, Bilian Yu^{2,†}, Qingrun Li^{1,†}, Yanhong Guo^{3,†}, Tomonari Koike³, Yui Koike³, Qingqing Wu¹, Jifeng Zhang³, Ling Mao², Xiaoyu Tang², Liang Sun⁴, Xu Lin⁴, Jiarui Wu^{1,5}, Y. Eugene Chen^{3,*}, Daoquan Peng^{2,*}, and Rong Zeng^{1,5,*}

¹ CAS Key Laboratory of Systems Biology, CAS Center for Excellence in Molecular Cell Science, Shanghai Institute of Biochemistry and Cell Biology, Chinese Academy of Sciences, Shanghai 200031, China

² Department of Cardiovascular Medicine, the Second Xiangya Hospital, Central South University, Changsha 410011, China

³ Department of Internal Medicine, Cardiovascular Center, University of Michigan Medical Center, Ann Arbor, MI 48109, USA

⁴ Key Laboratory of Nutrition and Metabolism, Shanghai Institute of Nutrition and Health, Chinese Academy of Sciences, Shanghai 200031, China

⁵ CAS Key Laboratory of Systems Biology, Hangzhou Institute for Advanced Study, University of Chinese Academy of Sciences, Chinese Academy of Sciences, Hangzhou 310024, China

[†] These authors contributed equally to this work.

* Correspondence to: Y. Eugene Chen, E-mail: echenum@med.umich.edu; Daoquan Peng, E-mail: pengdq@csu.edu.cn; Rong Zeng, E-mail: zr@sibs.ac.cn

Edited by Wei-Ping Jia

Lipoprotein, especially high-density lipoprotein (HDL), particles are composed of multiple heterogeneous subgroups containing various proteins and lipids. The molecular distribution among these subgroups is closely related to cardiovascular disease (CVD). Here, we established high-resolution proteomics and lipidomics (HiPL) methods to depict the molecular profiles across lipoprotein (Lipo-HiPL) and HDL (HDL-HiPL) subgroups by optimizing the resolution of anion-exchange chromatography and comprehensive quantification of proteins and lipids on the omics level. Furthermore, based on the Pearson correlation coefficient analysis of molecular profiles across high-resolution subgroups, we achieved the relationship of proteome–lipidome connectivity (PLC) for lipoprotein and HDL particles. By application of these methods to high-fat, high-cholesterol diet-fed rabbits and acute coronary syndrome (ACS) patients, we uncovered the delicate dynamics of the molecular profile and reconstruction of lipoprotein and HDL particles. Of note, the PLC features revealed by the HDL-HiPL method discriminated ACS from healthy individuals better than direct proteome and lipidome quantification or PLC features revealed by the Lipo-HiPL method, suggesting their potential in ACS diagnosis. Together, we established HiPL methods to trace the dynamics of the molecular profile and PLC of lipoprotein and even HDL during the development of CVD.

Keywords: HDL, high resolution, proteomics, lipidomics, atherosclerotic disease

Introduction

Lipoprotein particles play essential roles in lipid metabolism and energy homeostasis (Hoofnagle and Heinecke, 2009; Rye and Barter, 2014), and thus were closely related to metabolic disorders, such as obesity, diabetes, and atherosclerotic disease (cardiovascular disease, CVD) (Davidsson et al., 2005;

Lee et al., 2005; Hiukka et al., 2009; Vaisar et al., 2010, 2015; Riwanto et al., 2013). High-density lipoprotein (HDL) particles have many cardioprotective effects, including reverse cholesterol transport and inhibition of vascular inflammation (Barter and Rye, 2017). The distinct protein and lipid compositions in HDL subgroups were shown to be responsible for the diversity of HDL functions (Shepherd et al., 1978; Davidson et al., 2009; Wiesner et al., 2009; Gordon et al., 2010; Rothblat and Phillips, 2010). For example, the protein distribution across HDL subgroups is changed in type 2 diabetes and atherosclerosis, which severely influences the atheroprotective function of HDL (Swertfeger et al., 2017; Zhu et al., 2018). Therefore, robust and high-resolution methods should

Received July 15, 2021. Revised November 2, 2021. Accepted November 3, 2021.
© The Author(s) (2022). Published by Oxford University Press on behalf of *Journal of Molecular Cell Biology*, CEMCS, CAS.

This is an Open Access article distributed under the terms of the Creative Commons Attribution-NonCommercial License (<https://creativecommons.org/licenses/by-nc/4.0/>), which permits non-commercial re-use, distribution, and reproduction in any medium, provided the original work is properly cited. For commercial re-use, please contact journals.permissions@oup.com

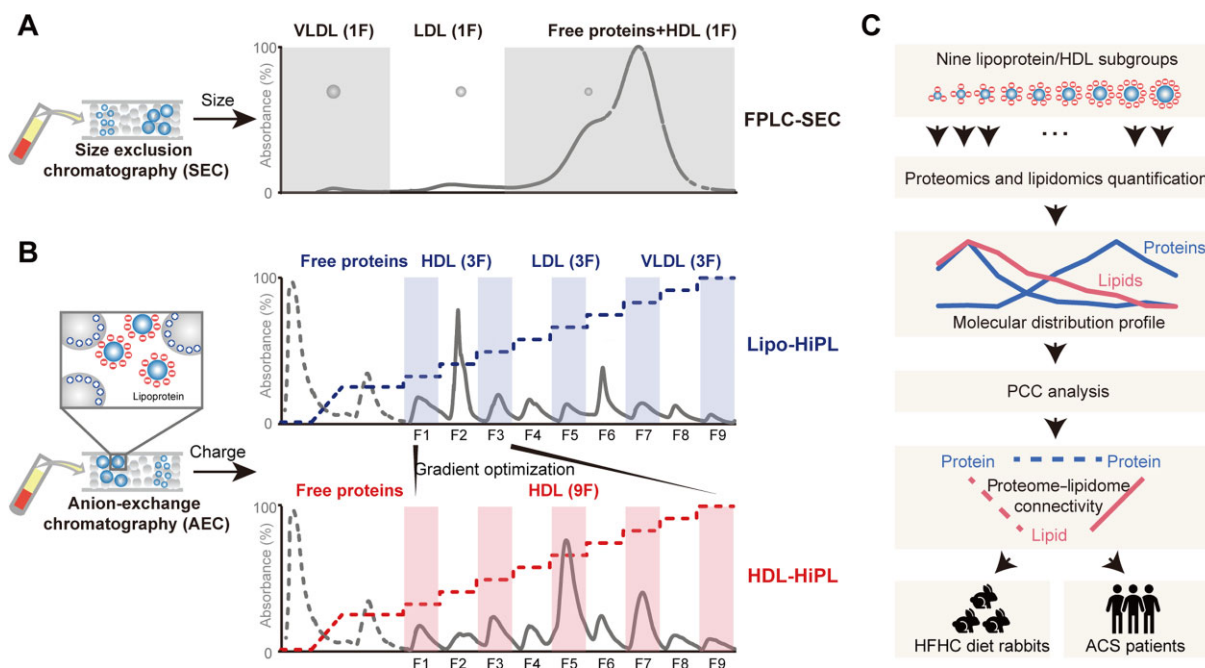


Figure 1 The workflow of the Lipo-HiPL and HDL-HiPL methods. **(A)** Traditional FPLC-SEC separates lipoprotein particles into three rough fractions (HDL, LDL, and VLDL). **(B)** The Lipo-HiPL and HDL-HiPL methods separate lipoprotein and HDL into nine high-resolution subgroups, respectively. To give a brief and overview picture of our HiPL method, the chromatographic peaks (280 nm) cover only a part of the retention time (from 20 min to 80 min) where the major lipoproteins elute out, and the absorbance (%) is the UV trace normalized by the maximum value. F, the abbreviation of fractions throughout the entire study. Dotted lines in blue and red show a gradient of elution phase. See Supplementary Figure S1C for the entire and raw UV traces. **(C)** Schematic diagram of the calculation of PLC. Proteins and lipids in each fraction were quantified by mass spectrometry. Based on the quantitative profile of each protein or lipid, PLC was calculated by the PCC analysis.

be applied to delicately separate the HDL subclasses. Moreover, the molecular profile dynamics during the progression of CVD need to be explored deeply by omics strategies (Gordon et al., 2013a).

However, to date, there are limited high-resolution separation methods to isolate lipoprotein and HDL subclasses. Ultracentrifugation is a sample-, time-, and labor-consuming method (Havel et al., 1955; Kunitake and Kane, 1982; van't Hooft and Havel, 1982). Besides, due to the poor resolution, size exclusion chromatography on fast performance liquid chromatography (FPLC-SEC) often results in the HDL fraction being contaminated by abundant free plasma proteins (Wiesner et al., 2009; Gordon et al., 2010). In comparison, anion-exchange chromatography (AEC) is a promising method to segregate lipoprotein subclasses with high resolution and reproducibility. Five major lipoprotein classes could be resolved by AEC according to their charge difference (Hirowatari et al., 2003). With fine optimization, we hypothesize that the AEC method can separate lipoproteins in a higher resolution and depict the in-depth landscape of the proteomics and lipidomics for lipoproteins.

Here, by application and optimization of AEC and mass spectrometry, we established high-resolution proteomics and lipidomics (HiPL) methods for effective separation and quantification of total lipoprotein (Lipo-HiPL) and HDL (HDL-HiPL) subgroups. Meanwhile, the method provided us the opportunity to study the proteome–lipidome connectivity (PLC) by the colo-

calization of the molecular profile across these subgroups, and thus trace the reconstruction of lipoprotein and HDL particles in high-fat, high-cholesterol (HFHC) diet-fed rabbits and acute coronary syndrome (ACS) patients. Notably, the PLC features revealed by the HDL-HiPL method could distinguish healthy individuals and ACS patients better than direct quantification of proteome and lipidome in HDL and low-density lipoprotein (LDL), and even better than PLC features revealed by the Lipo-HiPL method. In general, at the omics level under both physiological and pathological conditions, HiPL methods following Pearson correlation coefficient (PCC) analyses are robust and useful tools to trace the molecular profile and PLC of lipoprotein and HDL particles with high resolution.

Results

Optimization of AEC resolution for lipoprotein and HDL separation

Traditional FPLC-SEC separated lipoprotein particles into three rough fractions (HDL, LDL, and very low-density lipoprotein (VLDL)), and the HDL was contaminated with free plasma proteins (Figure 1A). Although the AEC method was capable of isolating lipoproteins into five classes (HDL, LDL, intermediate-density lipoprotein, VLDL, and chylomicron), the resulting HDL was still contaminated with free proteins with high abundance (mainly albumin) (Hirowatari et al., 2003). Therefore, we first optimized the AEC method by adding an elution step to

isolate free high-abundant proteins before HDL was eluted out (Supplementary Figure S1A). On the basis of the ratio of APOA1 to ALB, the elution gradient at 10% could maximize the purity of HDL without more HDL accumulating into the fraction of free high-abundant proteins (Supplementary Figure S1B, Tables S1 and S2). Next, to improve the AEC resolution for lipoprotein, we conducted the gradient elution with nine steps (eight steps from 13% to 37.5% with stepwise 3.5% and one step at 100%) to separate lipoprotein into nine fractions (Lipo-HiPL method) (Figure 1B; Supplementary Figure S1C). In addition, to further improve the resolution for HDL, we fine-tuned the elution gradient for HDL in the Lipo-HiPL method into nine moderate steps (from 11% to 19% with stepwise 1%). In this way, we could collect nine HDL fractions (HDL-HiPL method) (Figure 1B; Supplementary Figure S1C). Following high-resolution separation, proteins in each fraction were labelled with quantitative isobaric tandem mass tags (TMT10plex) and quantified by mass spectrometry. Meanwhile, the lipid extracts were identified and quantified using a targeted lipidomics method. The MRM list contained lipid classes of cholesteryl ester (CE), sphingomyelin (SM), ceramides (CER), dihydroceramide (DCER), hexosylceramide (HCER), lactosylceramide (LCER), triglyceride (TAG or TG), diglyceride (DAG), monoglyceride (MAG), phosphatidylcholine (PC), phosphatidylethanolamine (PE), phosphatidylglycerol (PG), phosphatidylinositol (PI), phosphatidylserine (PS), phosphatidic acid (PA), lyso-PC, lyso-PE, lyso-PG, lyso-PI, lyso-PS, and lyso-PA. While the Lipo-HiPL method could depict the whole picture of total lipoproteins in detail, the HDL-HiPL method could trace the molecular profile of HDL particles with a higher resolution. Importantly, with the quantitative profiling of each protein and lipid across nine fractions separated by the Lipo-HiPL and HDL-HiPL methods, we could construct the protein–protein and the protein–lipid distribution correlation by PCC analysis, namely PLC (Figure 1C).

The Lipo-HiPL and HDL-HiPL methods separate lipoprotein and HDL into high-resolution subgroups

To evaluate the performance of the Lipo-HiPL and HDL-HiPL methods, we separated plasma from five healthy individuals into nine fractions, respectively. In total, we quantified 347 proteins and 2848 peptides in all fractions separated by the Lipo-HiPL method (Supplementary Tables S3 and S4). The molecular profiles suggested that the fractions 1–3 contained most components from HDL, such as APOA1, APOA2, and PC, while the fractions 4–6 and 7–9 were dominated by the molecules derived from LDL and VLDL, respectively, such as APOB and CE in LDL and APOB and TAG in VLDL (Wiesner et al., 2009; Figure 2A; Supplementary Figure S2). Evidently, the distributions of other apolipoproteins were also consistent with that in the previous study (Wiesner et al., 2009; Hoofnagle et al., 2010; Gordon et al., 2013b; Figure 2B), suggesting the reliability of the molecular profiles revealed by the Lipo-HiPL method. To further confirm the separation reliability, we obtained ‘pre-purified HDL’ by the traditional SEC-FPLC for the Lipo-HiPL method. As expected, the extracted HDL was mainly eluted out in the first

three fractions, supporting that the fractions 1–3 bona fide were of the HDL components (Supplementary Figure S3). Of note, the profile correlation coefficients of APOA1, APOA2, and APOB were all >0.98 among three repetitive separations of the same plasma sample. For all quantified proteins and lipids, the correlation of >80% molecules was >0.75 (Figure 2C; Supplementary Figure S4, Tables S5 and S6), which further suggests the stability and repeatability of the Lipo-HiPL method. Among the total 208 proteins stably quantified (quantified in at least three individuals) by our Lipo-HiPL method (Supplementary Table S7), 98 hits (nearly half) were classified into lipoprotein particles by Gene Ontology cellular component (GO CC) analysis (Figure 2D). The high ratio (47%) of lipoprotein-associated proteins to total identified proteins in this study outperformed the previous report by FPLC (38%) (Swertfeger et al., 2017; Supplementary Figure S5). These results together proved that the Lipo-HiPL method was reliable, reproducible, and with high resolution for separation of total lipoprotein.

Compared with the Lipo-HiPL method, the HDL-HiPL method dedicatedly separated HDLs into nine fractions with a higher resolution. In total, we quantified 298 proteins and 2205 peptides in all fractions separated by the HDL-HiPL method (Supplementary Tables S8 and S9). As expected, HDL components, such as APOA1 and APOA2, were enriched, but the LDL and VLDL components, such as APOB, were undetectable in these nine HDL fractions (Figure 2A). Intriguingly, HDL fractions seemed to be subdivided into two main subgroups, named HDL I and HDL II, according to the profile of APOA1 and APOA2 (Figure 2A). For lipidomics, PC also showed a weak bimodal distribution turning at the fraction 4, while CE was found to be enriched in fraction 4. These results indicated that the HDL-HiPL method could effectively separate HDL into heterogeneous fractions with different protein–lipid compositions.

The Lipo-HiPL method traces the reconstruction of lipoprotein particles in rabbits during the HFHC diet

HFHC diet could trigger the development of atherosclerosis partly due to lipoprotein dysfunction (Waqar et al., 2010), especially in the rabbit model. Thus, plasma collected before (Pre) and after the HFHC diet (4W, 4 weeks; 8W, 8 weeks; and 14W, 14 weeks) of the rabbit model were studied by our Lipo-HiPL method (Figure 3A). In total, we quantified 462 proteins and 4086 peptides in all fractions separated by the Lipo-HiPL method (Supplementary Tables S10 and S11). Although the atherosclerotic lesions in the right coronary artery occurred until 19 weeks after HFHC induction (Figure 3B), noticeable changes of lipoproteins could be detected by the Lipo-HiPL method with high sensitivity as early as 4 weeks after HFHC induction. Chromatographically, the absorbance of peaks in LDL and VLDL fractions was obviously increased during the HFHC diet (Figure 3A). In accordance with the HDL dynamics in the physiological index (Figure 3C), APOA1 was decreased in the HDL fractions at 4W, flattened at 8W, and further down-regulated at 14W by the Lipo-HiPL method (Figure 3D). Significantly, some molecules displayed a similar increase with

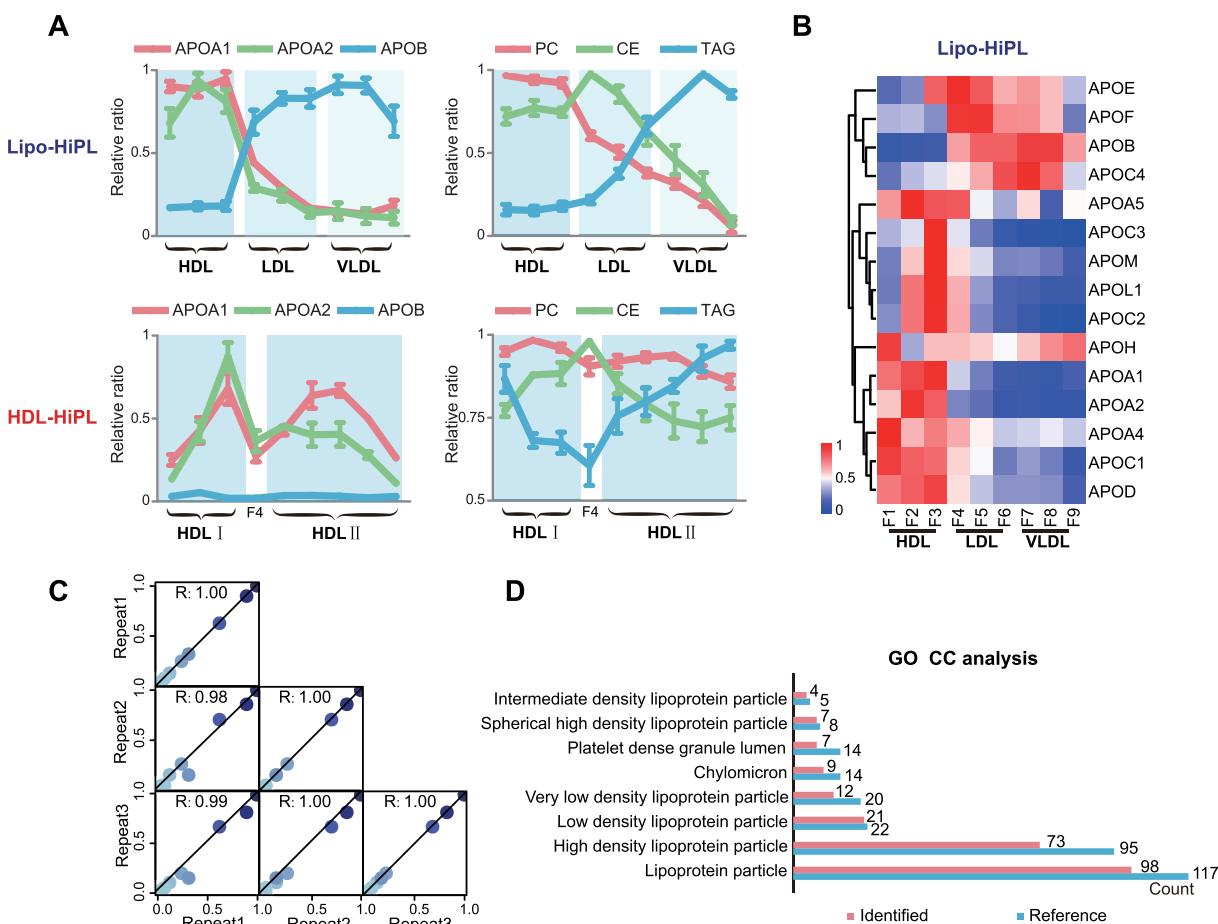


Figure 2 Separation performance assessment of the Lipo-HiPL and HDL-HiPL methods. **(A)** Profiles of APOA1, APOA2, APOB, and the three main lipid classes (PC, CE, and TAG) in nine fractions separated by the Lipo-HiPL and HDL-HiPL methods (healthy individual; $n = 5$; error bar: SEM). The relative ratio represents the ratio of apolipoprotein in each fraction normalized to the maximum ratio of this apolipoprotein (Lipo-HiPL) or three apolipoproteins (HDL-HiPL) in nine fractions. The relative ratio of the lipid class represents the ratio of lipid class normalized to the maximum ratio of this lipid class in nine fractions. See Supplementary material for the detailed calculation process of the relative ratios for proteins and lipids. **(B)** Distribution of apolipoproteins in nine lipoprotein fractions separated by the Lipo-HiPL method. The mean value of five healthy individuals was used. **(C)** APOA1 profile correlation among three repeats. The plasma pool of five healthy individuals was separated and quantified by the Lipo-HiPL method three times. The darker the blue, the higher is the relative ratio. **(D)** GO CC analysis of identified proteins in lipoprotein classes separated by the Lipo-HiPL method. Reference: a mixed database with 97 highly credible lipoprotein-related proteins in HDL and LDL watch lists summarized by Davidson lab (<http://homepages.uc.edu/~davidswm/HDLproteome.html>) combined with the GO database.

APOB, such as APOE, charged multivesicular body protein 4a (CHMP4A), and prenylcysteine oxidase 1 (PCYOX1). In contrast, others showed a similar decline with APOA1, such as APOM, adipocyte plasma membrane-associated protein (APMAP), and phosphatidylinositol-glycan-specific phospholipase D (GPLD1) (Figure 3D). The sharp dynamics of these molecules suggested their important role in the lipoprotein dysfunction induced by the HFHC diet. In addition, some molecules were shown to shift from HDL to LDL and VLDL fractions even if they had no significant changes in the total plasma level, such as APMAP and GPLD1, implying that the Lipo-HiPL method could track more elaborate dynamics for molecules (Supplementary Figure S6). Evidence showed that 90% of GPLD1 located on the APOA1- or APOA2-

containing lipoproteins (i.e. HDL) in normal physiological state (Cardner et al., 2020), which was consistent with the GPLD1 distribution profile at Pre in Figure 3D. GPLD1 can hydrolyze the GPI anchors of several inflammatory membrane proteins (e.g. CD106, CD55, and CD59) and has been suggested to regulate inflammation in atherosclerosis (O'Brien et al., 1999). Previous study revealed that GPLD1 was detected almost exclusively in atherosclerotic lesions and not in nonatherosclerotic areas (O'Brien et al., 1999). Since the deposition of LDL is an essential factor for the occurrence of atherosclerosis, our observation of the distribution shift of GPLD1 from HDL to LDL and VLDL might provide inspiration for the source of GPLD1 in atherosclerotic lesions.

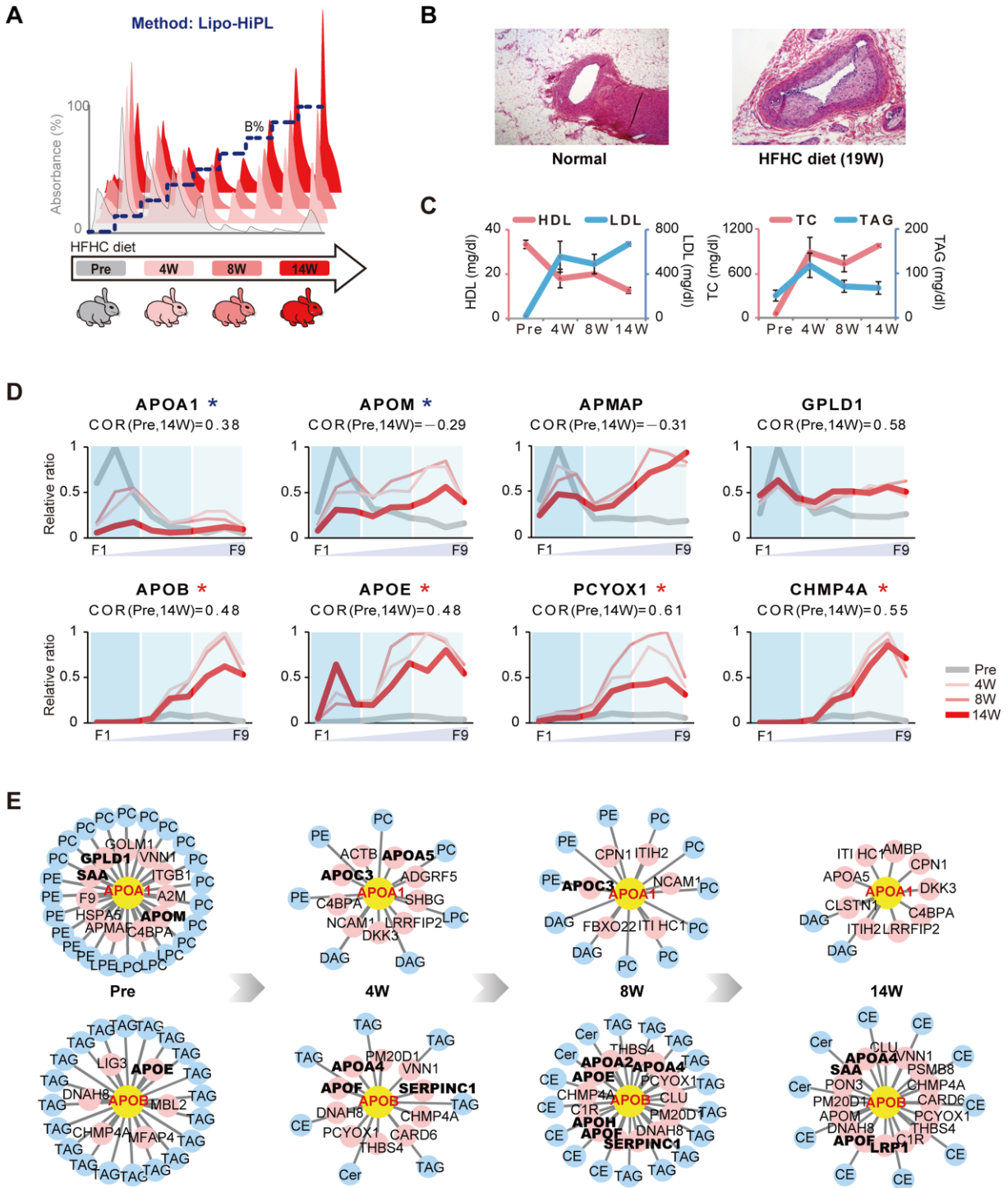


Figure 3 Molecular profile shift and PLC analysis of HFHC rabbits by the Lipo-HiPL method. **(A)** Lipoprotein separation chromatograms of rabbits before (Pre) and 4 weeks (4W), 8 weeks (8W), and 14 weeks (14W) after HFHC diet. **(B)** Coronary lesions in the right coronary artery in rabbits after 19 weeks of HFHC diet. **(C)** Absolute quantification change of total cholesterol (TC), TAG, HDL, and LDL during the HFHC diet ($n = 3$; error bar: SEM). **(D)** Molecular profile dynamics in rabbits during the HFHC diet. The relative ratio of a protein represents the ratio of the protein in each fraction normalized to the maximum ratio of this protein in all fractions of all groups. Each point represents the average relative ratio of three individual samples. $*P < 0.05$; the red asterisk stands for upregulation and the blue asterisk stands for downregulation at 14W in total plasma level, and the three shadows cover the HDL, LDL, and VLDL fractions, respectively. **(E)** Interactome dynamics of APOA1 and APOB during the HFHC diet based on PLC by PCC analysis. $PCC > 0.85$; proteins highlighted in black and bold are confirmed by the STRING database.

A previous study has proposed the protein correlation profiling strategies that proteins located in the same organelle have similar quantitative distributions among multiple fractions (Andersen et al., 2003). Following this principle, we constructed APOA1 and APOB interactomes based on PLC of the molecular profile across nine lipoprotein fractions. The Lipo-HiPL method clearly traced the remodeling of these interactomes, suggesting the reconstruction of lipoprotein particles during the HFHC diet (Figure 3E). In Pre state, the interactomes were in a steady condition, in which APOA1 strongly correlated with PC and a group of proteins (such as APOM, SAA, and GPLD1); meanwhile, APOB was associated with TAG and another group of proteins (such as APOE, DNAH8, and CHMP4A) (Figure 3E). Unexpectedly, all the interactomes were almost disrupted at 4W and set out to rebuild from 8W. During this process, the correlation of CE lipids with APOB was strengthened after the HFHC diet, and TAG lipids in the APOB interactome were thoroughly replaced by CE at 14W (Figure 3E). Particularly, PCYOX1, VNN1, and PM20D1 dramatically rose in LDL and VLDL fractions after the HFHC diet (Supplementary Figure S6), making them finally come into the APOB interactome at 14W (Figure 3E). The critical role of these molecules in the development of atherosclerosis further confirmed the reliability of the Lipo-HiPL method (see Supplementary Discussion for details). Additionally, the weak connectivity of APOA1 with other molecules at 14W suggested that the HDL components were severely disturbed by HFHC induction. Together, all these results suggested that the Lipo-HiPL method could accurately reflect the dynamics of the molecular profile and the reconstruction of HDL, LDL, and VLDL components during the HFHC diet.

The HDL-HiPL method reflects the reconstruction of HDL particles in ACS patients

ACS is the acute phase of myocardial ischemia, which is induced mainly by lipoprotein disorder (Alwaili et al., 2012). In order to evaluate the lipoprotein dysfunction in ACS patients, plasma from 15 ACS patients was collected within 24 h after the onset of chest pain. Another 15 healthy individuals, matched in age, gender, and clinical indexes (HDL-C, LDL-C, TC, and TG) with ACS patients, were selected to collect plasma as the healthy control (HC) (Supplementary Table S12). The plasma lipoprotein particles of these two groups were analyzed by the Lipo-HiPL and HDL-HiPL methods for whole lipoprotein and HDL profiling, respectively (Figure 4A). In total, we quantified 492 proteins and 3879 peptides in all fractions separated by the Lipo-HiPL method (Supplementary Tables S13 and S14) and 554 proteins and 3731 peptides by the HDL-HiPL method (Supplementary Tables S15 and S16). Compared with the obvious molecular profile change in rabbits during the HFHC diet, the Lipo-HiPL method revealed only a slight difference of lipoprotein between HC and ACS patients. For example, HDL components, such as APOA1 and APOA2, were mildly reduced, while LDL components, such as APOB and CHMP4A, were slightly increased in ACS patients (Figure 4B). Accordingly, the APOA1 interactome based on PLC in the Lipo-HiPL method showed inconspicuous changes between

HC and ACS patients (Figure 4C; Supplementary Table S17). Also, 76 proteins and 55 lipids were changed ($P < 0.05$) in lipoprotein fractions of ACS compared with HC by the Lipo-HiPL method (Supplementary Figure S7). However, 40 proteins and 59 lipids with the undetectable difference in the Lipo-HiPL method were found to be remarkably varied in HDL fractions using our higher-resolution HDL-HiPL method (Supplementary Figure S8). For example, APOC1 and APOD displayed no changes in the profiles by the Lipo-HiPL method, but were significantly decreased in the HDL I subclass by the HDL-HiPL method (Figure 4B). The slight dynamics of APOA1 and APOA2 in HDL fractions by the Lipo-HiPL method were obviously enlarged in the HDL I subclass by the HDL-HiPL method (Figure 4B). The HDL-HiPL method revealed enhanced connectivity of APOA1 with other molecules compared with HC (Figure 4C; Supplementary Table S18), suggesting the intense reconstruction of HDL particles in ACS. Previous studies have revealed that the composition and structure of HDL particles were remodeled in patients with ACS, e.g. the HDL proteome in ACS was shown to shift to an inflammatory profile (Alwaili et al., 2012). Similarly, our data showed that APOA1 correlated with multiple inflammation factors in ACS patients, such as GC, ORM2, CD44, and C1R. These findings evidently indicated that the HDL-HiPL method could accurately reflect the dynamics of molecular profiles and correlations in ACS patients.

Furthermore, although the changes were more dramatic in HFHC rabbits than in ACS patients, there were some molecules sharing similar dynamic patterns between HFHC rabbits (14W) and ACS patients (Figure 4D). For example, except the similar dynamics of APOA1, APOB, and CHMP4A as we discussed previously, PON1 decreased whereas APOC3, APOC4, GPLD1, and SAA1 rose in LDL/VLDL fractions in both HFHC rabbits and ACS patients, indicating their functional relevance in the development of CVD (see Supplementary Discussion for details).

PLC features revealed by the HDL-HiPL method are critical for ACS diagnosis

Considering the uniqueness of the APOA1 interactome based on PLC revealed by the HDL-HiPL method in ACS patients (Figure 4C), we supposed that the total PLC features revealed by the HDL-HiPL method (HDL-PLC) could effectively distinguish ACS patients from HC. To test this hypothesis, total HDL-PLC features were used for the classification of HC and ACS groups. As a comparison, Lipo-PLC features, as well as HDL and LDL features revealed by direct quantification of proteome and lipidome, were also used for the parallel classification of HC and ACS groups. To avoid the interference of other risk factors, we ensured that there was no significant difference in relevant clinical indicators (HDL-C, LDL-C, TC, and TG) between ACS and HC (Figure 5A). Unfortunately, either by direct quantification of proteome and lipidome or by Lipo-PLC features, one ACS patient was mixed up with the HC cluster in the classification results by HDL and LDL features (Figure 5B–D). Considering that the data-filtering method has great effect on the hierarchical cluster analysis (HCA) result, we also performed HCA using differential molecules in HDL and LDL with $P < 0.05$ and fold change 1.5 cutoff and

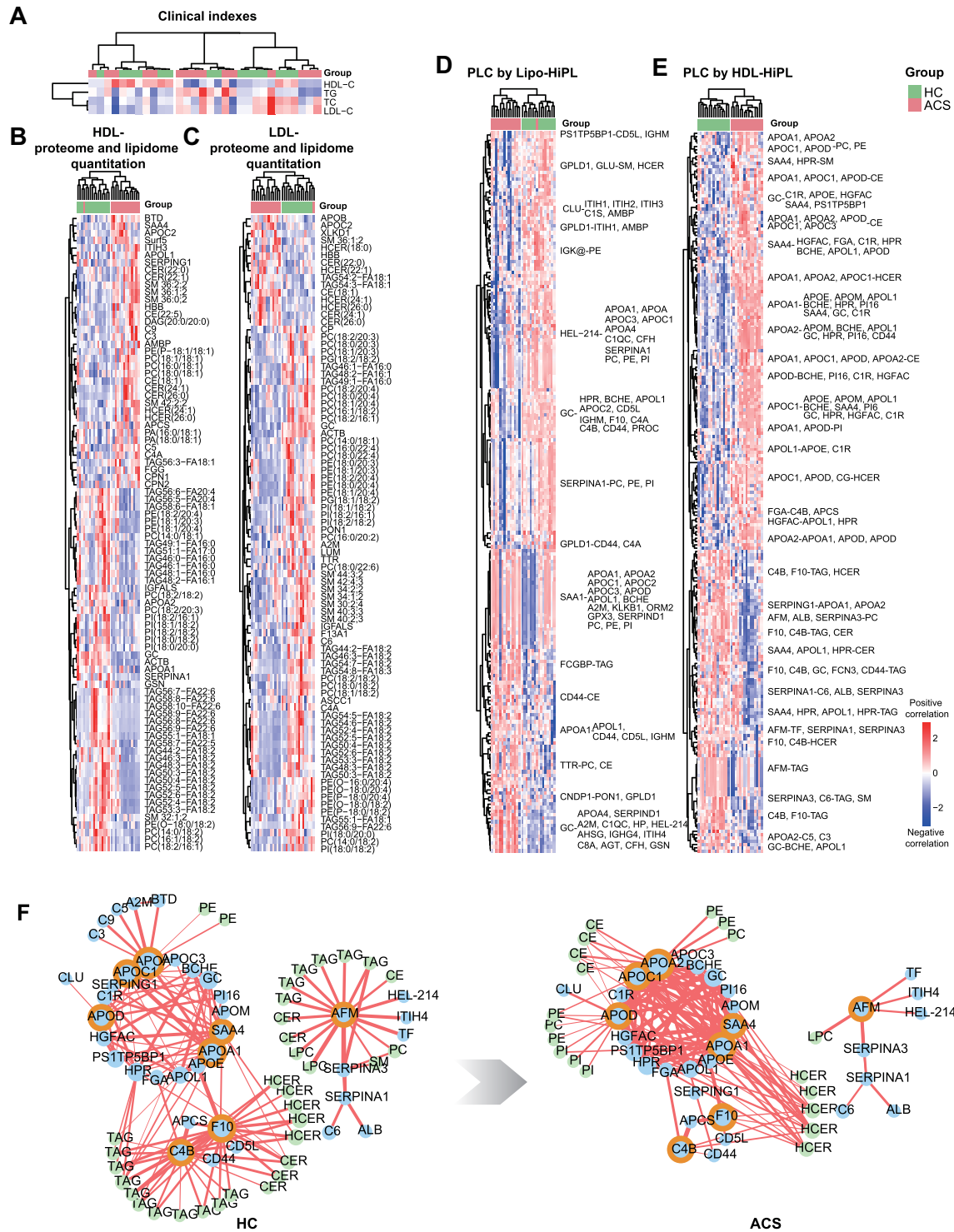


Figure 5 HCA of HC and ACS groups. (A–E) HCA using clinical indexes (HDL-C, LDL-C, TC, and TG) (A), differential quantitation of proteome and lipidome in HDL (B) and LDL (C) (P -value < 0.05 for proteins, P -value < 0.01 for lipids), and PLC features by the Lipo-HiPL (D) and HDL-HiPL (E) methods. Clustering_distance_column = ‘correlation’, clustering_distance_row = ‘correlation’, clustering_method = ‘complete’. See statistical analysis for the details of PLC feature screening. (F) Molecular networks of PLC features by the HDL-HiPL method. PCC > 0.5 for protein–protein interactions; PCC > 0.3 for protein–lipid interactions; the thicker the edge, the stronger is the association; blue and green nodes stand for proteins and lipids, respectively, and the orange-circled nodes are hubs whose degree is >18.

using the total quantified molecules (Supplementary Figure S9). The results showed that these methods could not contribute to the better classification.

In comparison, all ACS patients could be successfully discriminated from HC by HDL-PLC features (Figure 5E). The improved classification performance using HDL-PLC features was further confirmed by principle component analysis (Supplementary Figure S10). In addition, by constructing the correlation network based on HDL-PLC features, we found that the connectivity among a group of proteins became stronger in ACS than in HC (Figure 5F). Noticeably, we found that almost all hubs in this protein subnetwork were family proteins of apolipoproteins. As examples, we presented the accurate dynamic changes of the connectivities among hubs in the protein subnetwork (Supplementary Figure S11). APOA1, APOC1, SAA4, and APOD shared a similar profile shift with APOA2, moving from HDL I to HDL II in ACS patients, which led to their correlation coefficient increasing from 0.7 to >0.9. Together, these results stated clearly that the HDL-PLC was critical to show the dysfunction features of HDL in ACS patients and promising in ACS diagnosis.

Discussion

By high-resolution AEC separation and omics quantification, we were able to profile a variety of lipoprotein and HDL sub-species involving heterogeneous protein and lipid compositions. Though traditional ultracentrifugation was considered to be the reference of lipoprotein separation and enough to divide HDL into two major subclasses (HDL2 and HDL3) (Chapman et al., 1981), the large-scale clinical application suffered from the labor-intensive and time-consuming procedures. In comparison, SEC-FPLC was actually of poor resolution, with only one HDL chromatographic peak (Zhang et al., 2019). Previous studies have separated HDL into six subclasses bearing different median particle sizes by SEC-FPLC (Davidson and Shah, 2019). However, HDL was still presented to be a single peak according to the APOA1 distribution profile (Gordon et al., 2010). The distribution peaks of HDL subgroups by the Gaussian curve fitting technique severely overlapped with each other (Okazaki and Yamashita, 2016), which indicated that the resolution of SEC-FPLC was limited to achieve better separation. By AEC, HDL displayed a bimodal pattern corresponding to two major HDL particles, which was similar to ultracentrifugation. Considering the high heterogeneity of the protein–lipid composition in the nine fractions, there were potentially more subclasses in these two major HDL particles. The present AEC-based HiPL method not only could obtain high resolution better than ultracentrifugation, but also could be fast and with less sample consumption for clinical application. In addition, most of the previous omics work on lipoprotein particle analyses only focused on either proteome or lipidome (Okazaki and Yamashita, 2016; Davidson and Shah, 2019; Zhang et al., 2019). Considering the complexity of HDL particle composition, the integration of proteome and lipidome by our HiPL pipeline could demonstrate the most comprehensive and accurate characterization for lipoproteins and HDL particles.

The HFHC diet rendered an acute and apparent perturbation of lipid metabolism in rabbits, resulting in dramatic changes in the size, shape, and composition of lipoproteins (Hirowatari et al., 2012; Takeda et al., 2015; Xu et al., 2015). Unexpectedly, our Lipo-HiPL method could susceptibly reveal abundant molecular translocation among lipoprotein fractions in HFHC-challenged rabbits far earlier than the changes of pathophysiological index occur (Figure 3). Since the lipoprotein alterations between ACS patients and HCs would not be as dramatic as those found in rabbits, the high resolution and sensitivity of the HDL-HiPL method could deliver more delicate HDL alteration than the Lipo-HiPL method. For example, the proteins APOA1, APOA2, APOC1, and APOD significantly decreased in the HDL I subclass, and their distribution co-migrated from HDL I to HDL II in ACS when compared with HC (Figure 3).

More importantly, HiPL methods could provide molecular connectivity in lipoprotein particles, based on the protein–protein and protein–lipid distribution correlation. Similar distribution patterns of proteins and lipids across lipoprotein fractions indicated that they might reside on the same particles. In the current study, unlike the traditional analysis on a single component, HiPL methods allowed us to construct the PLC in each subject and reveal the lipoprotein or HDL features for ACS patients. Importantly, HDL-PLC features showed the best performance to evaluate lipoprotein dysfunction in ACS patients compared with other methods, such as LDL and HDL features by molecular quantification and Lipo-PLC features (Figure 5; Supplementary Figure S10). In the network based on HDL-PLC features, we found enhanced connectivity among a group of proteins in ACS patients (Figure 5F). The HDL-PLC not only contained quantitative information of proteins and lipids, but also indicated the spatial distribution as well as their functional interactions. Moreover, the HDL-PLC was expected to be more stable and reproducible than a single molecular feature across multiple samples. In general, the HDL-PLC could effectively evaluate HDL features, which is a promising indicator for CVD prognosis and diagnosis. Finally, these HDL-PLC features need to be further investigated in larger cohorts and by additional functional studies.

Materials and methods

The data, analytic methods, and study materials are available to other researchers for purposes of reproducing the results or replicating the procedure. An overview of the study design is shown in Figure 1. For full details of methods, please see Supplementary material.

Animals and diet

Sixteen-week-old male New Zealand white rabbits (male) were obtained from Covance. The rabbits were housed in a specific pathogen-free animal house at 24°C and a 12-h light/12-h dark cycle and were fed with either a chow diet or diet containing 0.3% cholesterol and 3% soybean oil (cholesterol-rich diet, 150 g/day) with free access to water ($n = 3$ for each group). Randomization and allocation concealment were performed. Blinding was performed in animal studies. Animals were fasted

overnight before the blood samples were collected. Rabbit studies were performed according to animal protocols approved by the Institutional Animal Care and Use Committee (IACUC) of the University of Michigan.

Study patients

A total of 15 patients undergoing acute ST-segment elevation myocardial infarction, which is the most severe type of ACS, were included in this study. Blood samples were collected within 24 h after the onset of chest pain. Fifteen HCs were matched in age, sex, and correlated clinical indexes (HDL-C, LDL-C, TC, and TG). Exclusion criteria were accompanying advanced kidney or liver failure, inflammatory, infectious or autoimmune disorders, neoplastic disorders, and a history of major surgery or trauma within the last 3 months. The study was approved by the Medical Ethics Committee of the Second Xiangya Hospital of Central South University. All patients gave written informed consent before blood sample collection.

Lipoprotein and HDL subdivision

A volume of 30 μ l plasma for each sample was used for AEC lipoprotein separation on the HPLC workstation UltiMate 3000 (Thermo Fisher Scientific). The separation was accomplished using an analytical 4.6 mm ID \times 3.5 cm TSK column fitted with a 4.6 mm ID \times 5 mm TSK pre-guard column from Tosoh. Buffer A was HPLC-grade water containing Tris-HCl (pH 7.5, 50 mM) and Na₂EDTA (1 mM). Buffer B was buffer A containing NaClO₄ (500 mM). Both buffers were purged for 5 min prior to use. The flow rate was held constant at 0.5 ml/min. Each fraction was collected by 2 min and, finally, every three adjacent fractions were combined into one. To divide lipoproteins into nine fractions, the ionic strength of the elution buffer was altered by changing buffer B% as follows: (1) hold buffer B% constant at 0% for 5 min; (2) increase buffer B% from 0% to 10% linearly over 5 min; (3) hold buffer B% constant at 10% for 10 min; (4) hold buffer B% constant in turn at 13%, 16.5%, 20%, 23.5%, 27%, 30.5%, 34%, 37.5%, and 41% (each for 6 min); (5) increase buffer B% to 100% over 5 min; (6) hold buffer B% constant for 5 min to wash the column; and (7) reduce buffer B% to 0% and hold constant for 5 min to regenerate the column. For the Lipo-HiPL method for humans, the fractions eluted at 41% and 100% were merged into one to result in the final nine fractions. For the Lipo-HiPL method for rabbits, the fractions were collected from 16.5% gradient to obtain the nine lipoprotein fractions.

To subdivide HDL into nine fractions, the buffer B% for step (4) was set as follows: hold buffer B% constant in turn at 11%, 12%, 13%, 14%, 15%, 16%, 17%, 18%, 19%, and 20% each for 6 min. The last two fractions keeping buffer B% at 20% and 100% were dropped, and nine HDL fractions were analyzed.

Proteomics and lipidomics data

Proteomics and lipidomics data were acquired by liquid chromatography–tandem mass spectrometry as detailed in Supplementary Methods.

Statistical analysis

The Shapiro–Wilk test was used to test the normality of data. To get the differentially expressed molecules, we compared the molecular quantification values of two groups (Pre against 14W for HFHC rabbits; HC against ACS for ACS patients) by the Wilcoxon test. Molecules with *P*-values < 0.05 (after Benjamini–Hochberg correction) were selected as differentially expressed molecules. The PCC analysis was used to construct molecular networks based on the quantitative profile of proteins and lipids across nine fractions separated by the Lipo-HiPL and HDL-HiPL methods. We calculated lipoprotein and HDL networks, respectively, for each subject in HC and ACS groups. In total, we have 30 networks for each HiPL method. We chose the differential edges (PLC features) for each method as follows: nodes (proteins and lipids) whose degree (molecule number correlated with this node, $PCC > 0.75$) significantly differed between HC and ACS ($P < 0.05$) were chosen; edges containing nodes with significantly different correlation between HC and ACS ($P < 0.05$) were chosen; and only edges containing proteins ($PCC > 0.5$ for protein–protein, $PCC > 0.3$ for protein–lipid) were chosen. The PCC cutoffs of these edges were chosen as a compromise between enabling molecular pairs to be correlated and significantly differential molecular pairs to be successfully selected (in our experience, a cutoff > 0.75 was too high to select the differential molecular pairs with strong correlation (> 0.75) in one group and weak correlation (< 0.75) in another group). Hubs were nodes whose degrees were > 18 .

Since the HDL-HiPL method with a higher resolution could detect the subtle profile difference, the molecular correlations across the nine lipoprotein fractions by the Lipo-HiPL method were generally higher than those across the nine HDL fractions by the HDL-HiPL method. APOA1 and APOB interactomes in Figure 3 were constructed using the correlations across the nine lipoprotein fractions. Thus, we appropriately increased the cut-off from 0.75 to 0.85 on the premise of not affecting the overall interactome dynamics.

R version 3.1.0 (<http://www.R-project.org/>) was used for all the statistical analyses. The raw mass spectrometry data and the search result files have been uploaded to the iProX database (project ID: IPX0003462000).

Supplementary material

Supplementary material is available at *Journal of Molecular Cell Biology* online.

Acknowledgements

The authors thank lab members from Chen, Peng, and Zeng Laboratories for insightful discussions.

Funding

This work was supported by a grant from the Strategic CAS Project (XDB38000000) and a grant from the National Natural Science Foundation of China (81561128018).

Conflict of interest: none declared.

References

- Alwalli, K., Bailey, D., Awan, Z., et al. (2012). The HDL proteome in acute coronary syndromes shifts to an inflammatory profile. *Biochim. Biophys. Acta* 1821, 405–415.
- Andersen, J.S., Wilkinson, C.J., Mayor, T., et al. (2003). Proteomic characterization of the human centrosome by protein correlation profiling. *Nature* 426, 570–574.
- Barter, P.J., and Rye, K.A. (2017). HDL cholesterol concentration or HDL function: which matters? *Eur. Heart J.* 38, 2487–2489.
- Cardner, M., Yalcinkaya, M., Goetze, S., et al. (2020). Structure–function relationships of HDL in diabetes and coronary heart disease. *JCI Insight* 5, e131491.
- Chapman, M.J., Goldstein, S., Lagrange, D., et al. (1981). A density gradient ultracentrifugal procedure for the isolation of the major lipoprotein classes from human serum. *J. Lipid Res.* 22, 339–358.
- Davidson, W.S., and Shah, A.S. (2019). High-density lipoprotein subspecies in health and human disease: focus on type 2 diabetes. *Methodist DeBakey Cardiovasc. J.* 15, 55–61.
- Davidson, W.S., Silva, R.A., Chantepie, S., et al. (2009). Proteomic analysis of defined HDL subpopulations reveals particle-specific protein clusters: relevance to antioxidative function. *Arterioscler. Thromb. Vasc. Biol.* 29, 870–876.
- Davidsson, P., Hulthe, J., Fagerberg, B., et al. (2005). A proteomic study of the apolipoproteins in LDL subclasses in patients with the metabolic syndrome and type 2 diabetes. *J. Lipid Res.* 46, 1999–2006.
- Gordon, S.M., Davidson, W.S., Urbina, E.M., et al. (2013a). The effects of type 2 diabetes on lipoprotein composition and arterial stiffness in male youth. *Diabetes* 62, 2958–2967.
- Gordon, S.M., Deng, J.Y., Lu, L.J., et al. (2010). Proteomic characterization of human plasma high density lipoprotein fractionated by gel filtration chromatography. *J. Proteome Res.* 9, 5239–5249.
- Gordon, S.M., Deng, J.Y., Tomann, A.B., et al. (2013b). Multi-dimensional co-separation analysis reveals protein–protein interactions defining plasma lipoprotein subspecies. *Mol. Cell. Proteomics* 12, 3123–3134.
- Havel, R.J., Eder, H.A., and Bragdon, J.H. (1955). The distribution and chemical composition of ultracentrifugally separated lipoproteins in human serum. *J. Clin. Invest.* 34, 1345–1353.
- Hirowatari, Y., Kon, M., Shimura, Y., et al. (2012). Anion-exchange HPLC separation of five major rabbit lipoproteins using a nonporous diethylaminoethyl-ligated gel with a perchlorate-containing eluent. *Biomed. Chromatogr.* 26, 434–440.
- Hirowatari, Y., Yoshida, H., Kurosawa, H., et al. (2003). Measurement of cholesterol of major serum lipoprotein classes by anion-exchange HPLC with perchlorate ion-containing eluent. *J. Lipid Res.* 44, 1404–1412.
- Hiukka, A., Stahlman, M., Pettersson, C., et al. (2009). ApoCIII-enriched LDL in type 2 diabetes displays altered lipid composition, increased susceptibility for sphingomyelinase, and increased binding to biglycan. *Diabetes* 58, 2018–2026.
- Hoofnagle, A.N., and Heinecke, J.W. (2009). Lipoproteomics: using mass spectrometry-based proteomics to explore the assembly, structure, and function of lipoproteins. *J. Lipid Res.* 50, 1967–1975.
- Hoofnagle, A.N., Vaisar, T., Mitra, P., et al. (2010). HDL lipids and insulin resistance. *Curr. Diab. Rep.* 10, 78–86.
- Kunitake, S.T., and Kane, J.P. (1982). Factors affecting the integrity of high density lipoproteins in the ultracentrifuge. *J. Lipid Res.* 23, 936–940.
- Lee, C.Y., Lesimple, A., Larsen, A., et al. (2005). ESI-MS quantitation of increased sphingomyelin in Niemann-Pick disease type B HDL. *J. Lipid Res.* 46, 1213–1228.
- O'Brien, K.D., Pineda, C., Chiu, W.S., et al. (1999). Glycosylphosphatidylinositol-specific phospholipase D is expressed by macrophages in human atherosclerosis and colocalizes with oxidation epitopes. *Circulation* 99, 2876–2882.
- Okazaki, M., and Yamashita, S. (2016). Recent advances in analytical methods on lipoprotein subclasses: calculation of particle numbers from lipid levels by gel permeation HPLC using ‘Spherical Particle Model’. *J. Oleo Sci.* 65, 265–282.
- Riwanto, M., Rohrer, L., Roschitzki, B., et al. (2013). Altered activation of endothelial anti- and proapoptotic pathways by high-density lipoprotein from patients with coronary artery disease: role of high-density lipoprotein-proteome remodeling. *Circulation* 127, 891–904.
- Rothblat, G.H., and Phillips, M.C. (2010). High-density lipoprotein heterogeneity and function in reverse cholesterol transport. *Curr. Opin. Lipidol.* 21, 229–238.
- Rye, K.A., and Barter, P.J. (2014). Regulation of high-density lipoprotein metabolism. *Circ. Res.* 114, 143–156.
- Shepherd, J., Patsch, J.R., Packard, C.J., et al. (1978). Dynamic properties of human high density lipoprotein apoproteins. *J. Lipid Res.* 19, 383–389.
- Swertfeger, D.K., Li, H., Rebholz, S., et al. (2017). Mapping atheroprotective functions and related proteins/lipoproteins in size fractionated human plasma. *Mol. Cell. Proteomics* 16, 680–693.
- Takeda, H., Koike, T., Izumi, Y., et al. (2015). Lipidomic analysis of plasma lipoprotein fractions in myocardial infarction-prone rabbits. *J. Biosci. Bioeng.* 120, 476–482.
- Vaisar, T., Mayer, P., Nilsson, E., et al. (2010). HDL in humans with cardiovascular disease exhibits a proteomic signature. *Clin. Chim. Acta* 411, 972–979.
- Vaisar, T., Tang, C., Babenko, I., et al. (2015). Inflammatory remodeling of the HDL proteome impairs cholesterol efflux capacity. *J. Lipid Res.* 56, 1519–1530.
- van't Hooft, F., and Havel, R.J. (1982). Metabolism of apolipoprotein E in plasma high density lipoproteins from normal and cholesterol-fed rats. *J. Biol. Chem.* 257, 10996–11001.
- Waqar, A.B., Koike, T., Yu, Y., et al. (2010). High-fat diet without excess calories induces metabolic disorders and enhances atherosclerosis in rabbits. *Atherosclerosis* 213, 148–155.
- Wiesner, P., Leidl, K., Boettcher, A., et al. (2009). Lipid profiling of FPLC-separated lipoprotein fractions by electrospray ionization tandem mass spectrometry. *J. Lipid Res.* 50, 574–585.
- Xu, J., Jullig, M., Middleditch, M.J., et al. (2015). Modelling atherosclerosis by proteomics: molecular changes in the ascending aortas of cholesterol-fed rabbits. *Atherosclerosis* 242, 268–276.
- Zhang, Y., Gordon, S.M., Xi, H., et al. (2019). HDL subclass proteomic analysis and functional implication of protein dynamic change during HDL maturation. *Redox. Biol.* 24, 2213–2317.
- Zhu, X., Shah, A.S., Swertfeger, D.K., et al. (2018). High-density lipoproteins-associated proteins and subspecies related to arterial stiffness in young adults with type 2 diabetes mellitus. *Complexity* 2018, 1–14.